IEEE Access
Multidisciplinary : Rapid Review : Open Access Journal

Received November 4, 2019, accepted November 11, 2019, date of publication November 19, 2019, date of current version December 4, 2019.

Digital Object Identifier 10.1109/ACCESS.2019.2954281

Towards Debris Information Analysis and Abstraction for Wi-Fi Radar Edge in Collapsed Structures

MUHAMMAD FAIZAN KHAN[1], GUOJUN WANG[1], (Member, IEEE), AND MD. ZAKIRUL ALAM BHUIYAN[2], (Senior Member, IEEE)
[1]School of Computer Science, Guangzhou University, Guangzhou 510006, China
[2]Department of Computer and Information Sciences, Fordham University, New York, NY 10458, USA

Corresponding author: Guojun Wang (csgjwang@gzhu.edu.cn)

This work was supported in part by the National Natural Science Foundation of China under Grant 61632009 and Grant 61472451, in part by the Guangdong Provincial Natural Science Foundation under Grant 2017A030308006, and in part by the High-Level Talents Program of Higher Education in Guangdong Province under Grant 2016ZJ01.

ABSTRACT Structural collapses are widespread, owing to a surge in climatic changes, earthquakes, and terrorism. Therefore, there are some technological rescue methods in practice that involve sensors, radars, cameras, microphones, and robots. However, deployment of these techniques faces at least one issue amongst cost, availability, and technical expertise, which limits their application in developing countries. So, there is a dire need for a low-cost and easy deployable rescue method. Recently, we witnessed an increasing trend of using Wi-Fi radios as sensing modality for various applications, including breathing detection and localization, thus leading to device-free communication. Based on this, we may envisage having a Wi-Fi rescue solution. However, Wi-Fi signals cannot easily penetrate through collapsed structures due to the multi-layered obstacle scenario. So, in this study, we focus our research on the proper information analysis and abstraction of debris and also present the possible methodology to have better coverage for Wi-Fi signals using Wi-Fi radar edge. We define two objectives of this work; 1) debris information analysis and 2) the Wi-Fi signal propagation mechanism, respectively. We achieve our first goal by conducting site surveys of earthquake-hit areas that enable us to analyze the causes and types of structural collapses followed by debris concept selection model. We employ a bijective soft set approach to accurately select the debris based on the complexity and nature of structural engineering followed. Moreover, we use the Wi-Fi Halow radar edge for wireless signal propagation and perform extensive simulations at low power. Finally, we compare both methods and discuss prospects.

INDEX TERMS Collapsed structure, coverage, debris, rescue, bijective soft set, Wi-Fi radar.

I. INTRODUCTION

Post-disaster rescue from collapsed structures using ubiquitous methods is getting more attention from the research community owing to the surge in climate changes, earthquakes, war, and terrorism [1]. According to studies [2], [3], the first 72 hours are very crucial for the survival of missing or trapped humans. Therefore, there are many rescue techniques in literature, such as robots, cameras, radars, and sensors, etc. However, cost and non-availability limit applications of these methods in developing countries. But, with the realization of leveraging Wi-Fi signals as sensing information [4], the research trend has shifted to widget free solutions in each domain, as these are readily available and deployable. However, these Wi-Fi signals are weak if subjected to penetration through collapsed structures for rescue. So, in this paper, we study the nature of debris and its proper modeling to address the weak Wi-Fi signal strength through a low-powered Wi-Fi radar approach.

A. PRIOR WORK AND MOTIVATION

We observe that natural and human-made phenomena such as climatic changes, earthquakes, fire, war, and terrorism can all cause the mounting frequency of disasters [5]. These disasters affect thousands or even millions of people every year, who

The associate editor coordinating the review of this manuscript and approving it for publication was Honghao Gao.

get missing or trapped because of the collapsed structures, ruptures, or any other incident. The key to rescue efforts is the survival time that declines sharply after 72 hours [2]. So, post-disaster rescue from collapsed structures has been extensively studied within the domain of social sciences, engineering, and computing [1]–[3], [5], [6].

Let us revisit the rescue techniques as most of the countries are still using manual methods. The most common methods being used today are robots [6], [7], and radars [8], but both are a bit expensive and are not available in developing countries, where unfortunately the majority of the structural damages occur. The other solutions are based on cameras [9], sensors [1], [10], [11], UAV's [12] and, biobots [13]. Similarly, NASA has developed radar device, "FINDER"[1] that can detect heartbeats under the debris. However, these techniques are not feasible due to cost, deployment, and the result. Let us discuss the drawbacks of these techniques, which eventually led us to study new methods. We observe that robots, UAV's, Biobots, and radar-based solutions like FINDER are not available in developing countries due to cost, and also unavailability within 72 hours, which is a major challenge. Furthermore, none of these except FINDER"[2] proved to be much successful in practical scenarios. Similarly, cameras and sensor-based solutions are cheap as the cost is an important factor in developing countries, but these methods still need plenty of cameras and sensor deployment in the disaster area, which is quite difficult considering the survival time. Also, there are multiple challenges to these cameras and sensors in the form of invisibility, noises, and hurdles. So, these have not been proved successful even because of low-cost. Therefore, there is dire need to have such rescue methods that should be cost-effective, easily deployable, and available in third world countries where most of the collapses occur due to poor constructions. So, this provides us room for more investigation in the subject matter.

Looking for potential rescue methods, we observed an increasing trend of leveraging Wi-Fi signals as the mode of sensing information other than mere internet backbone. These wireless signals have an interesting feature known as channel state information (CSI) [14], which encompasses all detail of the desired event happening in the surrounding. This has led to device-free sensing where signals contain all information hence truly revolutionizing the IoTs. Some of the most noticeable Wi-Fi sensing applications are; CSI-based indoor localization [15], RT-Fall [16], security [14], WiFi-ID [17], breathing detection [18], Mo-sleep [19], WiGest [20], and WiHear [21] to name a few. Let us discuss the feasibility of these Wi-Fi signal applications for rescue scenario as collapsed structures. We envision that breathing detection using Wi-Fi signals can be utilized for detecting the breath of alive ones under debris, which will be device-free, easily deployable, universally available, and cost-effective edge level rescue solution. However, locating the individuals in ruins is a big challenge. Although, there are applications using Wi-Fi signals for indoor localization yet those are not effective for collapsed structures owing to complex multilayered debris. Howsoever, this does provide us room to investigate more on the strength of Wi-Fi signals in debris scenarios because successful breathing detection can lead to device-free rescue solutions that would be cost-effective and available round the globe.

Let us consider the challenges to Wi-Fi signals in collapsed structures. The most significant issues are the complexity of debris and signal penetration from this multi-obstacle environment. Although, there are some studies [22], [23] that deal with various frequencies, i.e., [50MHz to 2.4GHz] in complex structures as attenuations, fading, scattering and improper reflections weaken the signal, but these do not consider Wi-Fi signals as sensing information. Moreover, path loss modeling has been extensively studied in [24]–[26], but none of these works explicitly deal with Wi-Fi signals penetration in collapsed structures. Similarly, we observe many studies in literature related to debris flow [27]–[29]. However, there is a significant room for investigation of collapsed structure debris in the context of Wi-Fi signals. To the best of our knowledge, no study explicitly deals with the nature, type, and impact of the static collapsed debris concerning wireless signals. Although, there are works by authors in [30]–[33], where they tried to investigate the feasibility of Wi-Fi signals for collapsed structures and suggested that Wi-Fi Halow [34] working with Wi-Fi radar technique can provide breakthrough towards Wi-Fi signals based rescue. However, we also did not conduct a proper analysis of the nature of static collapsed debris, which was a matter of great concern. So, in this study, we primarily focus on debris nature as our previous works were more inclined towards signal behavior.

B. CONTRIBUTION AND ORGANIZATION

We aim to study the nature, types, and impact of static collapsed structure debris on the Wi-Fi Halow signal. To meet our objective, we set two targets. Firstly, we need to develop a proper debris model based on real field surveys to have better analysis and selection of the most commonly used materials in construction. After that, we employ our Wi-Fi radar method to assess the Wi-Fi signal coverage through these materials for possible comparison and inference. To address these targets, we conducted two field surveys of earthquake-hit areas from two countries, i.e., China and Pakistan, as both disasters resulted in the loss of more than 160 thousand people combined. Furthermore, we conducted an investigation on the nature of the debris, buildings types, and construction materials found in these field surveys followed by layered and echo models to properly study Wi-Fi radar signals. Moreover, we present debris selection mechanism by employing bijective soft set theory [35], as it can provide us the best concept of construction materials that can be subject to Wi-Fi radar signal method for coverage computation. Finally, we simulate the debris concept for low-powered Wi-Fi Halow

[1] https://spinoff.nasa.gov/spinoff2018/ps_1.html

[2] https://www.nasa.gov/jpl/finder-search-and-rescue-technology-helped-save-lives-in-nepal

signals across various debris and signal parameters. After that, we compare the results with each other and discuss methodology with existing techniques to benchmark our work.

The major contributions of this study are;

- We study the nature of debris to have better coverage of Wi-Fi Halow signals. There are multiple causes of static collapsed debris, which are climatic changes, earthquake hazards, fire, war, and terrorism. We limit this study to earthquake debris and conducted field surveys in disaster-affected areas. Furthermore, we classify the debris types, materials, and discuss the soil mechanics and engineering standards followed as an inference from field surveys.
- We define our debris selection problem through collapsed building assessment and debris models followed by an echo model for Wi-Fi Halow signals. These conceptual models based on field surveys provide space for in-depth investigation of challenges encountered to Wi-Fi signals in collapsed structures. Moreover, the echo model entails Wi-Fi signals to work quite similar to the Doppler radar method, where reflections encompassing information are used for inference.
- We employ a bijective soft set theory method to transform debris and building assessment models into proper debris information analysis mechanism. This method is based on the selection of pivotal attributes that define the nature of collapsed buildings. We assign debris with the best and worst cases to figure out the maximum and minimum possible coverage while integrating it with the Wi-Fi radar technique.
- Finally, we perform extensive simulations while employing the Wi-Fi radar method at Wi-Fi Halow frequencies to validate the debris selection concept. The simulations results are verified across various signal intensities, debris complexity obtained through the bijective soft set, modulation schemes, thresholds, and limitations from standard bodies. We conclude that low-powered Wi-Fi Halow signals with medium debris case can still provide better coverage. However, coverage is very weak for worst-case debris, which convinces us to have advanced methods in the future. Howsoever, this study has significant contributions to the research community as it is first of its kind in this domain, which emphasizes that no matter how advanced coverage technique are we using, there is dire need to analyze the debris at first. Lastly, through this work, we can expect to have IoT based rescue solutions for what Wi-Fi Halow has been primarily designed.

We organize the remainder of this paper as follows; problem formulation is presented in Section II, whereas Section III discusses the methodology to deal with debris and building assessment model. Furthermore, we provide debris information analysis techniques such as bijective soft set and Wi-Fi radar in Sections IV and V, respectively. Afterward, simulations results have been provided in Section VI followed by performance analysis in Section VII. Finally, Section VIII concludes the paper with future directions.

II. PROBLEM FORMULATION

In this section, we lay bases of debris concept selection. We dissect the problem into subsections as; 1) presents the field surveys of two earthquake sites with analysis of the debris's nature, 2) provides the assessment of collapsed building types, 3) discusses the outcome of assessment models into layered debris model, and finally 4) introduces Wi-Fi echo model employing Wi-Fi radar method to study coverage in collapsed structures.

A. MEASUREMENT STUDIES

The first and foremost step towards debris concept selection is identifying the possible collapsed structure environment that causes much damage and is prevalent in most of the developing nations. There are multiple causes of disasters ranging from climatic changes, earthquakes, war, fire, and terrorism, to name a few. However, in this study, we limit ourselves to field surveys of earthquake sites. This is because of the active fault lines that exist mostly in developing countries, where construction standards and building codes are not followed adequately due to the weak economy. We conducted field studies of two different earthquake sites from China and Pakistan to have better consideration of debris owing to local traditions and culture as well.

1) WENCHUAN EARTHQUAKE STUDY

Let us consider our first field study. We surveyed Wenchuan county, located in southwestern China. The epic center of the earthquake was Yingxiu,[3] a small town in southern Wenchuan county located at latitude and longitude of 31°03'32'' N and 103° 29' 41'' E respectively, as shown in Fig 1a. Most of the adjoining rural areas of Wenchuan were destroyed by a devastating earthquake that hit China with a moment magnitude of 7.9 on May 12, 2008.[4] Government sources have indicated the number of casualties to more than 68,000.

We conducted a comprehensive investigation from the ruins of Xuankou Middle School, as shown in Fig 1b, in Yingxiu town. We observed that the structural collapse was triggered by the poor construction of concrete and bricks, and the non-structural elements were glass and lumber, as shown in Fig 1c. The collapse also created voids, which are free spaces under debris and can have humans trapped there. Therefore, appropriate studies comprising the causes of structural failure can lead to better rescue. Our analysis shows that the columns were unreliable, and the steel bonding in the core basement did not meet construction specifications. Even the beam did not reach the mark and was subject to

[3]https://en.wikipedia.org/wiki/Yingxiu

[4]https://earthquake.usgs.gov/earthquakes/eventpage/usp000g650#executive

(a) Location of Yingxiu town **(b)** Ruins of Xuankou middle school **(c)** Mapping collapsed materials

FIGURE 1. **Earthquake survey site 1: Yingxiu town, Wenchuan County, P.R. China.**

(a) Location of Balakot city **(b)** Ruins of central market **(c)** Mapping collapsed materials

FIGURE 2. **Earthquake survey site 2: Balakot City, KPK, Pakistan.**

collapse during the first shock. In short, weak construction materials with improper building codes were a major source of collapse.

2) BALAKOT EARTHQUAKE STUDY

Let us consider our second field study of Balakot,[5] which is a small town located at a latitude of 34.550842 and longitude of 73.352957, respectively in Mansehra district of Khyber-Pakhtunkhwa province, Pakistan, as shown in Fig 2a. On October 8, 2005, a devastating earthquake of magnitude 7.6 struck northern Pakistan, almost destroying this town.[6] According to official statistics from the Pakistani government, 87,350 people were killed, 138,000 injured, and 3.5 million became homeless.[7] The seismic fault line crosses the central market in Balakot[8]; therefore, it was severely ruined.

We conducted a thorough investigation of the damaged central plaza, as shown in Fig 2b. We observed that poor construction aggravated the severity of the damage, and resulted in a higher number of causalities in the affected areas. This central plaza was partially damaged owing to the poor construction of concrete and masonry blocks, and the non-structural elements were glass and wood, as shown in Fig 2c. We interacted with locals who informed us that voids allowed rescuers to save the trapped humans there. Furthermore, we had additional shocking findings as well, because Pakistan is a developing country, where a lack of experts and poor administration led to indecorous reconstruction. Most of the civil structures in the ostentatious region were weak wall construction based on non-engineered unreinforced masonry (URM) methods. As per our observation, these URM constructions were typically constituent of single or double stories of a solid concrete block, unreinforced solid brick or stone masonry-bearing walls with reinforced concrete floors, which were either pitched or flat. Furthermore, there were also flat roofs structure constituent of wood (non-machined) beams and straw-reinforced mud slabs in small adjoining villages. These weak structures are intermittently locally termed as "Tayyar Chath," which is made up of lightly reinforced concrete slabs or galvanized iron (GI) sheets.

[5]https://en.wikipedia.org/wiki/Balakot
[6]https://earthquake.usgs.gov/earthquakes/eventpage/usp000e12e#executive
[7]http://www.ndma.gov.pk/publications.php
[8]http://www.gsp.gov.pkpublication

B. COLLAPSED BUILDING ASSESSMENT MODELS

Let us have a proper assessment of collapsed buildings from our field surveys and literature review. We observe that each structural collapse has its specific characteristics. We can classify our assessment into four types of structural collapses for URM, as shown in Fig 3.

1) LEAN-TO COLLAPSE

Lean-to collapse occurs when one or more walls or floors break or separate from joints, which causes one to fall to the extreme and sojourn on the lower floor. This type of crack causes a triangular space where the chances of the victim's survival are high, as shown in Fig 3a. This debris is one of the safest types of collapsed structures.

2) V-SHAPED COLLAPSE

This type of collapse is caused by letting both sides of the floor remain intact. However, the floor is collapsed in an angle

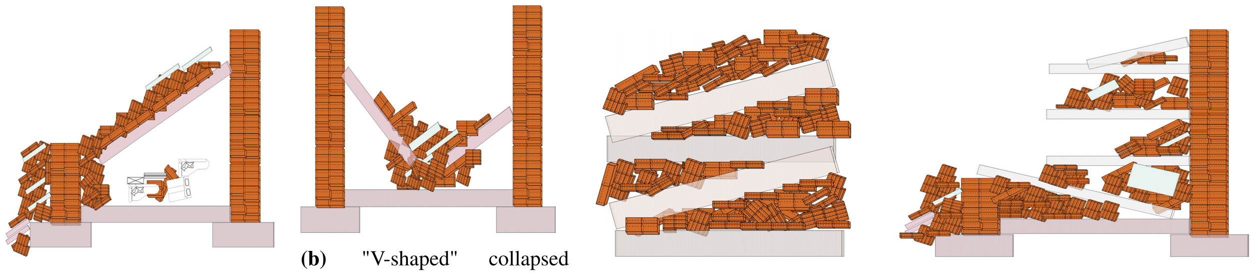

(a) Lean-to collapsed model (b) "V-shaped" collapsed model (c) Pancake collapsed model (d) Suspended ceilings collapsed model

FIGURE 3. Building collapsed models.

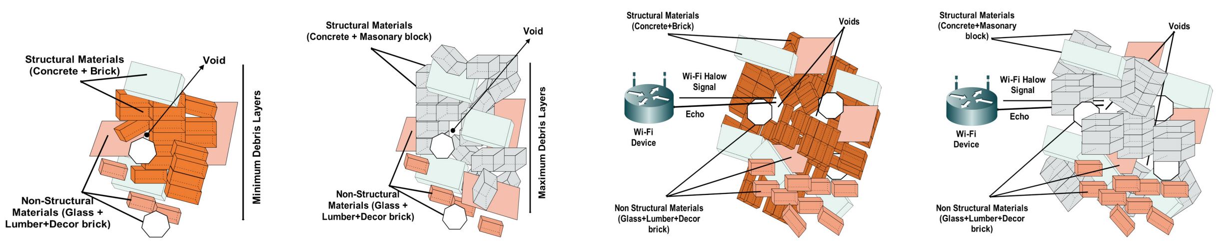

(a) Minimum layered debris (b) Maximum layered debris (c) Echo model for brick (d) Echo model for block

FIGURE 4. Debris modelling with layered and echo models for brick and masonary block materials.

with the lower part of standing walls quite similar to "V," as shown in Fig 3b. This collapsed type also creates voids from where humans can be rescued if trapped.

3) PANCAKE COLLAPSE

This type of collapse is caused by the complete failure of columns or load-bearing walls. Therefore, upper floors almost horizontally over the lower ones, as witnessed in Xuankou Middle School Fig 1c. Victims are buried under a higher volume of debris and have difficulty in taking a breath and can stay alive only for a shorter time. This type of collapse causes fewer voids and is much prevalent in concrete buildings, as shown in Fig 3c.

4) SUSPENDED COLLAPSE

The failure of walls causes this type of collapse, and one extreme of floors remain suspended in the air, whereas the other floor side is still connected with walls. We witnessed this type of collapse in Balakot central plaza, Fig 2b. Although, this collapse model, as shown in Fig 3d, causes voids where victims are trapped, yet it is difficult for them to remove suspended debris by themselves.

C. DEBRIS MODEL

In this part, we map inferences from field surveys and building assessment models to a conceptual layered debris model, as shown in Fig 4. We have already figured out the debris nature in preceding sections, which can be categorized into structural and non-structural materials. This selection of construction materials, along with the collapse type, plays a pivotal role in strengthening coverage of weak Wi-Fi signals in collapsed structures. We consider concrete, brick, masonry block as our structural materials, whereas lumber, glass, and decoration brick have been taken as non-structural materials.

Let us have a thorough analysis of our layered debris model. We classify it into a maximum and minimum layers' scenario. Moreover, the enclosed debris area is spread both horizontally and vertically. However, the horizontal spread is not a significant concern because humans are not trapped inside, whereas vertical layers will cause much damage. Therefore, our primary concern is vertical layers that are laying over each other as collapsed structure results results in a multi-layered obstacle scenario. We map minimum and maximum layered cases using brick and masonry block in Fig 4a and 4b, respectively. Let it be clear that bricks and masonry blocks are used in wall construction, and our field survey provided us insight that Pakistani construction is mostly based on masonry block. On the contrary, the Chinese field survey showed that brick was used in wall construction. So, we mapped both cases to have better study.

D. Wi-Fi RADAR ECHO MODEL

In this part, we map Wi-Fi Halow signals to the afore-proposed layered debris model in Fig 4. We observe that wireless signals penetrate through debris layers and are subject to reflections, scattering, fading, and damping. However, we envisage having reflected Wi-Fi signals that may have significant CSI owing to victims trapped in voids, which can further be used for breathing detection in future studies. In other words, our focus is an echo signal quite similar to Doppler radar that we can receive after all possible noises and obstructions from this multi-cluttered environment.

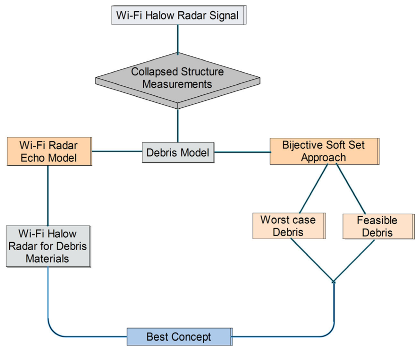

(a) Debris information analysis mechanism

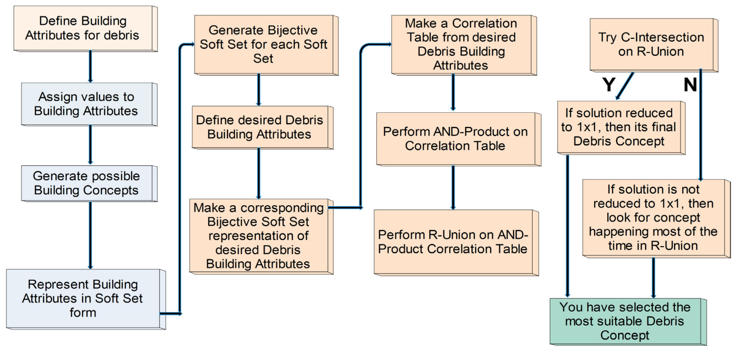

(b) Proposed functional concept methodology

FIGURE 5. Illustration of debris selection concept for Wi-Fi radar.

Moreover, we model this Wi-Fi echo concept in Fig 4c and 4d for both brick and masonry block debris cases.

Let it be known that layered debris massively weakens the Wi-Fi signal. However, there is still a possibility to receive strong reflected signals partially. So, to avoid aliasing and noise effects, we consider the minimum receivable signal and assign a pre-defined threshold (PTD) to it. Furthermore, we also assume signals other than reflected from debris as cluttered ones.

In a nutshell, we aim to study the debris nature and select the right materials to have significant coverage of Wi-Fi radar signals. Therefore, this is a dire need to explore techniques that may lead us to better understandings of debris in the context of Wi-Fi signals as sensing information for potential rescue in the future.

III. DEBRIS INFORMATION ANALYSIS

In this section, we briefly discuss the debris concept analysis mechanism. Firstly, the impact of debris study is analyzed that was driving force behind this work. After that, we succinctly elucidate the strategies to have proper debris selection and Wi-Fi coverage through selected materials.

The main goal of this study is to investigate the static collapsed debris in the context of Wi-Fi signals as sensing information. Authors suggested in their previous work [31] that low-powered and low-frequency Wi-Fi Halow signal can provide optimal coverage in collapsed structures. However, there was a limitation of proper debris modeling. To the best of our knowledge, there is no such study that explicitly deals with static collapsed debris. Therefore, we focus on Wi-Fi Halow signals for particular debris to exploit the CSI functionality for possible rescue.

Let us consider the strategies to study the debris concept selection and coverage of Wi-Fi Halow signals, as shown in Fig 5a. Firstly, there is a need to select proper debris that may be subject to wireless signals. There can be multiple ways to study the debris, but analytical approaches such as [36], [37] are the most suited ones owing to opinion-making and decision techniques. In the light of preceding sections, we employ a bijective soft set method [35] to select the best and worst-case debris. This method is based on attribute selections of an object under consideration, and then bijective soft sets are applied using AND and OR operation on correlation tables. These operations yield the desired debris concepts, which we need to be studied for Wi-Fi signal coverage. After that, we introduce our Wi-Fi radar method to pre-selected debris materials and type for optimal coverage. Furthermore, we compare various debris cases for Wi-Fi radar signals and select the best ones. Finally, a comparison is made with the bijective soft set method, which ensures the selection of the best debris case.

IV. BIJECTIVE SOFT SET METHOD

This section presents the debris concept information analysis technique. We employ a bijective soft set approach to address the debris nature, attributes, and coverage prospects. Firstly, we briefly discuss the motivation behind using this method from the operational sciences to computer research. Afterward, we present preliminaries that may assist in applying the method to our debris model.

Let us discuss the motivation behind employing a bijective soft set technique to debris selection problem. We observe that decision making from multi-criteria attributes associated with an object under consideration is a major challenge in operational sciences. We envision that debris selection is an operational problem because before deploying any solution, a proper decision is needed at forehand to achieve better results. To address the multi-criteria attributes problem, Molodtsov [38] introduced soft sets, which was extended to the bijective soft set by [39]. Afterward, intuitionistic fuzzy soft sets were discussed by [40]. We observe that soft sets in any form are best suited in operational research to deal with uncertainties and effective decision making such as [41], [42]. This provides us the motivation that soft sets can also be used in debris concept selection because after having a thorough field survey and debris modeling, there is a need to make proper decisions for debris nature. This method leads to effective Wi-Fi signal coverage modeling by yielding favorable results for rescue in the future. Therefore, we employ the bijective soft set method as Tiwari applied to a particular engineering problem in [35] to our debris model, as shown in Fig 5b.

Let us briefly discuss the bijective soft set mechanism. Firstly, we map the debris attributes of a collapsed building to soft sets. Afterward, a correlation table on the bijective soft set is constructed, where union and intersection operations are applied. These operations are applied both on rows and columns and labeled as Row Union(RUnion), Column Union(CUnion), Row Intersection(RIntersection), and Column Intersection(CIntersection), respectively as defined in [43]. Finally, this method yields the most suitable concept according to our needs, which is feasible debris in this case.

A. PRELIMINARY DEFINITIONS

We need to define and understand the fundamentals of bijective soft sets as subsequent sections become more understandable.

1) SOFT SET

Let us suppose M as a set of parameters and U to be universal set, respectively. Now, P(U) is the power set of U, and Y is a subset of M as Y ⊂ M. Then, a pair (SoS, Y) is known as a soft set over U, where mapping function SoS is given by SoS:Y → P(U) [43].

2) BIJECTIVE SOFT SET

Similarly, we consider (SoS, M) as a soft set over universal set U and M as a non-empty set of parameters. Then, (SoS, M) is known as bijective soft set [39] if the following conditions are met:

- i $\bigcup_{\Psi \in M} SoS(\Psi) = U$.
- ii For any two parameters;
  $\Psi_i, \Psi_j, \Psi_j \in M$, $\Psi_i = \Psi_j$, $\mathrm{SoS}(\Psi_i) \cap \mathrm{SoS}(\Psi_j) = \varnothing$.

B. METHOD

Input: Set of building functional attributes

Output: Best debris selection concept

1) Identify the building functional attributes because these are the core of debris. Assign the possible values to these attributes from building and earthquake engineering perspective.
2) Generate building concepts based on assessment and debris models for attribute values, which can be most suitable for debris selection in collapsed structures. This assortment ensures better coverage of Wi-Fi signals.
3) Represent attributes values in both soft and bijective soft set form for better decision making of debris.
4) Postulate desired debris attributes for best and worst scenarios. Make a corresponding soft set and bijective soft set representation of these debris cases.
5) Construct AND-Product correlation table by mapping the debris postulates. Denote it with k × k, where building attributes values in each set are represented by k.
6) Perform union operation on either row or column to reduce AND-product correlation table to 1 × k or k × 1.
7) Perform intersection operation on either column or row of R-union or C-Union and reduce the union correlation table to 1 × 1. This output is our desired debris concept. However, if the union table is not reduced to 1 × 1, then go to step 5, and select the most occurring concept.

C. OPERATION

Let us apply the bijective soft set approach to debris concept selection problem. It can be done as follows;

- i We solve the debris selection problem with identifying the building attributes, which are the most important for any structure to stand intact. Let us define building functional attributes(BAs) to form a set BA as per 1: $\mathcal{BA} = [\mathcal{BA}_1, \mathcal{BA}_2, \mathcal{BA}_3, \mathcal{BA}_4, \mathcal{BA}_5, \mathcal{BA}_6]$, where each attributes corresponds to;
  $\mathcal{BA}_1 = \mathcal{F}oundations$, $\mathcal{BA}_2 = \mathcal{E}xterior\ \ walls$, $\mathcal{BA}_3 = \mathcal{F}loor$, $\mathcal{BA}_4 = \mathcal{S}tructure$, $\mathcal{BA}_5 = \mathcal{I}nterior\ \ partition$, $\mathcal{BA}_6 = \mathcal{V}erticle\ \ systems$
  Furthermore, we assign values to these $\mathcal{BA}$s as per building and earthquake engineering perspective to deal with debris secanrio. We denote these values with υ as follows;
  $\mathcal{BA}_1 = \{\upsilon_{11}, \upsilon_{12}\} = \{Strong, Weak\}$
  $\mathcal{BA}_2 = \{\upsilon_{21}, \upsilon_{22}\} = \{Load\ bearing, Non\ load\ bearing\}$
  $\mathcal{BA}_3 = \{\upsilon_{31}, \upsilon_{32}\} = \{Heavy\ weight, Light\ weight\}$
  $\mathcal{BA}_4 = \{\upsilon_{41}, \upsilon_{42}\} = \{Strong, Weak\}$
  $\mathcal{BA}_5 = \{\upsilon_{51}, \upsilon_{52}\} = \{Heavy, Light\}$
  $\mathcal{BA}_6 = \{\upsilon_{61}, \upsilon_{62}\} = \{Strong, Weak\}$
- ii We generate six building concepts as per 2 by forming a debris applicable combination from $\mathcal{BA}$s, which can be presented in a universal set given as;
  $\bigcup = \mathcal{B}\zeta_1 + \mathcal{B}\zeta_2 + \mathcal{B}\zeta_3 + \mathcal{B}\zeta_4 + \mathcal{B}\zeta_5 + \mathcal{B}\zeta_6$
  We form following building concepts for debris selection;
  $\mathcal{B}\zeta_1 = \{\upsilon_{11}, \upsilon_{21}, \upsilon_{32}, \upsilon_{42}, \upsilon_{51}, \upsilon_{62}\}$
  $\mathcal{B}\zeta_2 = \{\upsilon_{11}, \upsilon_{21}, \upsilon_{31}, \upsilon_{42}, \upsilon_{51}, \upsilon_{61}\}$
  $\mathcal{B}\zeta_3 = \{\upsilon_{11}, \upsilon_{22}, \upsilon_{32}, \upsilon_{41}, \upsilon_{52}, \upsilon_{62}\}$
  $\mathcal{B}\zeta_4 = \{\upsilon_{12}, \upsilon_{21}, \upsilon_{32}, \upsilon_{42}, \upsilon_{51}, \upsilon_{62}\}$
  $\mathcal{B}\zeta_5 = \{\upsilon_{12}, \upsilon_{22}, \upsilon_{31}, \upsilon_{41}, \upsilon_{52}, \upsilon_{61}\}$
  $\mathcal{B}\zeta_6 = \{\upsilon_{12}, \upsilon_{22}, \upsilon_{32}, \upsilon_{41}, \upsilon_{51}, \upsilon_{62}\}$
- iii Now, let us present building attributes values in soft and bijective soft set form. Soft sets from $\mathcal{B}\zeta$ can be as follows; $(\mathcal{S}oS_1, \mathcal{BA}_1) = \{\mathcal{S}oS_1(\upsilon_{11}), \mathcal{S}oS_1(\upsilon_{12})\}$
  $(\mathcal{S}oS_2, \mathcal{BA}_2) = \{\mathcal{S}oS_2(\upsilon_{21}), \mathcal{S}oS_2(\upsilon_{22})\}$
  $(\mathcal{S}oS_3, \mathcal{BA}_3) = \{\mathcal{S}oS_3(\upsilon_{31}), \mathcal{S}oS_3(\upsilon_{32})\}$
  $(\mathcal{S}oS_4, \mathcal{BA}_4) = \{\mathcal{S}oS_4(\upsilon_{41}), \mathcal{S}oS_4(\upsilon_{42})\}$
  $(\mathcal{S}oS_5, \mathcal{BA}_5) = \{\mathcal{S}oS_5(\upsilon_{51}), \mathcal{S}oS_5(\upsilon_{52}))\}$
  $(\mathcal{S}oS_5, \mathcal{BA}_6) = \{\mathcal{S}oS_6(\upsilon_{61}), \mathcal{S}oS_6(\upsilon_{62}))\}$
  Furthermore, bijective soft sets as per 3 can be given as;
  $\mathcal{S}oS_1(\upsilon_{11}) = \{\mathcal{B}\zeta_1, \mathcal{B}\zeta_2, \mathcal{B}\zeta_3\}$;
  $\mathcal{S}oS_1(\upsilon_{12}) = \{\mathcal{B}\zeta_4, \mathcal{B}\zeta_5, \mathcal{B}\zeta_6\}$;
  $\mathcal{S}oS_2(\upsilon_{21}) = \{\mathcal{B}\zeta_1, \mathcal{B}\zeta_2, \mathcal{B}\zeta_4\}$;
  $\mathcal{S}oS_2(\upsilon_{22}) = \{\mathcal{B}\zeta_3, \mathcal{B}\zeta_5, \mathcal{B}\zeta_6\}$; $\mathcal{S}oS_3(\upsilon_{31}) = \{\mathcal{B}\zeta_2, \mathcal{B}\zeta_5\}$;
  $\mathcal{S}oS_3(\upsilon_{32}) = \{\mathcal{B}\zeta_1, \mathcal{B}\zeta_3, \mathcal{B}\zeta_4, \mathcal{B}\zeta_6\}$;
  $\mathcal{S}oS_4(\upsilon_{41}) = \{\mathcal{B}\zeta_3, \mathcal{B}\zeta_5, \mathcal{B}\zeta_6\}$;
  $\mathcal{S}oS_4(\upsilon_{42}) = \{\mathcal{B}\zeta_1, \mathcal{B}\zeta_2, \mathcal{B}\zeta_4\}$;
  $\mathcal{S}oS_5(\upsilon_{51}) = \{\mathcal{B}\zeta_1, \mathcal{B}\zeta_2, \mathcal{B}\zeta_4, \mathcal{B}\zeta_6\}$;

TABLE 1. ***AND*-Product correlation table: $\mathcal{DBA}_1$.**

$\{DBA\ \ Set\}$	Cr_{i1}	Cr_{i2}	Cr_{i3}	Cr_{i4}	Cr_{i5}	Cr_{i6}
Cr_{1j}	$SoS(\upsilon_{12}) \wedge SoS(\upsilon_{12})$	$SoS(\upsilon_{12}) \wedge SoS(\upsilon_{21})$	$SoS(\upsilon_{12}) \wedge SoS(\upsilon_{31})$	$SoS(\upsilon_{12}) \wedge SoS(\upsilon_{42})$	$SoS(\upsilon_{12}) \wedge SoS(\upsilon_{51})$	$SoS(\upsilon_{12}) \wedge SoS(\upsilon_{62})$
Cr_{2j}	$SoS(\upsilon_{21}) \wedge SoS(\upsilon_{12})$	$SoS(\upsilon_{21}) \wedge SoS(\upsilon_{21})$	$SoS(\upsilon_{21}) \wedge SoS(\upsilon_{31})$	$SoS(\upsilon_{21}) \wedge SoS(\upsilon_{42})$	$SoS(\upsilon_{21}) \wedge SoS(\upsilon_{51})$	$SoS(\upsilon_{21}) \wedge SoS(\upsilon_{62})$
Cr_{3j}	$SoS(\upsilon_{31}) \wedge SoS(\upsilon_{12})$	$SoS(\upsilon_{31}) \wedge SoS(\upsilon_{21})$	$SoS(\upsilon_{31}) \wedge SoS(\upsilon_{31})$	$SoS(\upsilon_{31}) \wedge SoS(\upsilon_{42})$	$SoS(\upsilon_{31}) \wedge SoS(\upsilon_{51})$	$SoS(\upsilon_{31}) \wedge SoS(\upsilon_{62})$
Cr_{4j}	$SoS(\upsilon_{42}) \wedge SoS(\upsilon_{12})$	$SoS(\upsilon_{42}) \wedge SoS(\upsilon_{21})$	$SoS(\upsilon_{42}) \wedge SoS(\upsilon_{31})$	$SoS(\upsilon_{42}) \wedge SoS(\upsilon_{42})$	$SoS(\upsilon_{42}) \wedge SoS(\upsilon_{51})$	$SoS(\upsilon_{42}) \wedge SoS(\upsilon_{62})$
Cr_{5j}	$SoS(\upsilon_{51}) \wedge SoS(\upsilon_{12})$	$SoS(\upsilon_{51}) \wedge SoS(\upsilon_{21})$	$SoS(\upsilon_{51}) \wedge SoS(\upsilon_{31})$	$SoS(\upsilon_{51}) \wedge SoS(\upsilon_{42})$	$SoS(\upsilon_{51}) \wedge SoS(\upsilon_{51})$	$SoS(\upsilon_{51}) \wedge SoS(\upsilon_{62})$
Cr_{6j}	$SoS(\upsilon_{62}) \wedge SoS(\upsilon_{12})$	$SoS(\upsilon_{62}) \wedge SoS(\upsilon_{21})$	$SoS(\upsilon_{62}) \wedge SoS(\upsilon_{31})$	$SoS(\upsilon_{62}) \wedge SoS(\upsilon_{42})$	$SoS(\upsilon_{62}) \wedge SoS(\upsilon_{51})$	$SoS(\upsilon_{62}) \wedge SoS(\upsilon_{62})$

TABLE 2. ***AND*-Product correlation table: $\mathcal{DBA}_1$.**

$\{\mathcal{DBA}\ \ Set\}$	Cr_{i1}	Cr_{i2}	Cr_{i3}	Cr_{i4}	Cr_{i5}	Cr_{i6}
Cr_{1j}	$\{\mathcal{B}\zeta_4, \mathcal{B}\zeta_5, \mathcal{B}\zeta_6\}$	$\{\mathcal{B}\zeta_4\}$	$\{\mathcal{B}\zeta_5\}$	$\{\mathcal{B}\zeta_4\}$	$\{\mathcal{B}\zeta_4, \mathcal{B}\zeta_6\}$	$\{\mathcal{B}\zeta_4, \mathcal{B}\zeta_6\}$
Cr_{2j}	$\{\mathcal{B}\zeta_4\}$	$\{\mathcal{B}\zeta_1, \mathcal{B}\zeta_2, \mathcal{B}\zeta_4\}$	$\{\mathcal{B}\zeta_2\}$	$\{\mathcal{B}\zeta_1, \mathcal{B}\zeta_2, \mathcal{B}\zeta_4\}$	$\{\mathcal{B}\zeta_1, \mathcal{B}\zeta_2, \mathcal{B}\zeta_4\}$	$\{\mathcal{B}\zeta_1, \mathcal{B}\zeta_4\}$
Cr_{3j}	$\{\mathcal{B}\zeta_5\}$	$\{\mathcal{B}\zeta_2\}$	$\{\mathcal{B}\zeta_2, \mathcal{B}\zeta_5\}$	$\{\mathcal{B}\zeta_2\}$	$\{\mathcal{B}\zeta_2\}$	$\{\}$
Cr_{4j}	$\{\mathcal{B}\zeta_4\}$	$\{\mathcal{B}\zeta_1, \mathcal{B}\zeta_2, \mathcal{B}\zeta_4\}$	$\{\mathcal{B}\zeta_2\}$	$\{\mathcal{B}\zeta_1, \mathcal{B}\zeta_2, \mathcal{B}\zeta_4\}$	$\{\mathcal{B}\zeta_1, \mathcal{B}\zeta_2, \mathcal{B}\zeta_4\}$	$\{\mathcal{B}\zeta_1, \mathcal{B}\zeta_4\}$
Cr_{5j}	$\{\mathcal{B}\zeta_4, \mathcal{B}\zeta_6\}$	$\{\mathcal{B}\zeta_1, \mathcal{B}\zeta_2, \mathcal{B}\zeta_4\}$	$\{\mathcal{B}\zeta_2\}$	$\{\mathcal{B}\zeta_1, \mathcal{B}\zeta_2, \mathcal{B}\zeta_4\}$	$\{\mathcal{B}\zeta_1, \mathcal{B}\zeta_2, \mathcal{B}\zeta_4, \mathcal{B}\zeta_6\}$	$\{\mathcal{B}\zeta_1, \mathcal{B}\zeta_4, \mathcal{B}\zeta_6\}$
Cr_{6j}	$\{\mathcal{B}\zeta_4, \mathcal{B}\zeta_6\}$	$\{\mathcal{B}\zeta_1, \mathcal{B}\zeta_4\}$	$\{\}$	$\{\mathcal{B}\zeta_1, \mathcal{B}\zeta_4\}$	$\{\mathcal{B}\zeta_1, \mathcal{B}\zeta_4, \mathcal{B}\zeta_6\}$	$\{\mathcal{B}\zeta_1, \mathcal{B}\zeta_3, \mathcal{B}\zeta_4, \mathcal{B}\zeta_6\}$

TABLE 3. ***AND*-Product correlation table: $\mathcal{DBA}_2$.**

$\{DBA\ \ Set\}$	Cr_{i1}	Cr_{i2}	Cr_{i3}	Cr_{i4}	Cr_{i5}	Cr_{i6}
Cr_{1j}	$SoS(\upsilon_{11}) \wedge SoS(\upsilon_{11})$	$SoS(\upsilon_{11}) \wedge SoS(\upsilon_{22})$	$SoS(\upsilon_{11}) \wedge SoS(\upsilon_{32})$	$SoS(\upsilon_{11}) \wedge SoS(\upsilon_{41})$	$SoS(\upsilon_{11}) \wedge SoS(\upsilon_{52})$	$SoS(\upsilon_{11}) \wedge SoS(\upsilon_{61})$
Cr_{2j}	$SoS(\upsilon_{22}) \wedge SoS(\upsilon_{11})$	$SoS(\upsilon_{22}) \wedge SoS(\upsilon_{22})$	$SoS(\upsilon_{22}) \wedge SoS(\upsilon_{32})$	$SoS(\upsilon_{22}) \wedge SoS(\upsilon_{41})$	$SoS(\upsilon_{22}) \wedge SoS(\upsilon_{52})$	$SoS(\upsilon_{22}) \wedge SoS(\upsilon_{61})$
Cr_{3j}	$SoS(\upsilon_{32}) \wedge SoS(\upsilon_{11})$	$SoS(\upsilon_{32}) \wedge SoS(\upsilon_{22})$	$SoS(\upsilon_{32}) \wedge SoS(\upsilon_{32})$	$SoS(\upsilon_{32}) \wedge SoS(\upsilon_{41})$	$SoS(\upsilon_{32}) \wedge SoS(\upsilon_{52})$	$SoS(\upsilon_{32}) \wedge SoS(\upsilon_{61})$
Cr_{4j}	$SoS(\upsilon_{41}) \wedge SoS(\upsilon_{11})$	$SoS(\upsilon_{41}) \wedge SoS(\upsilon_{22})$	$SoS(\upsilon_{41}) \wedge SoS(\upsilon_{32})$	$SoS(\upsilon_{41}) \wedge SoS(\upsilon_{41})$	$SoS(\upsilon_{41}) \wedge SoS(\upsilon_{52})$	$SoS(\upsilon_{41}) \wedge SoS(\upsilon_{61})$
Cr_{5j}	$SoS(\upsilon_{52}) \wedge SoS(\upsilon_{11})$	$SoS(\upsilon_{52}) \wedge SoS(\upsilon_{22})$	$SoS(\upsilon_{52}) \wedge SoS(\upsilon_{32})$	$SoS(\upsilon_{52}) \wedge SoS(\upsilon_{41})$	$SoS(\upsilon_{52}) \wedge SoS(\upsilon_{52})$	$SoS(\upsilon_{52}) \wedge SoS(\upsilon_{61})$
Cr_{6j}	$SoS(\upsilon_{61}) \wedge SoS(\upsilon_{11})$	$SoS(\upsilon_{61}) \wedge SoS(\upsilon_{22})$	$SoS(\upsilon_{61}) \wedge SoS(\upsilon_{32})$	$SoS(\upsilon_{61}) \wedge SoS(\upsilon_{41})$	$SoS(\upsilon_{61}) \wedge SoS(\upsilon_{52})$	$SoS(\upsilon_{61}) \wedge SoS(\upsilon_{61})$

TABLE 4. ***AND*-Product correlation table: $\mathcal{DBA}_2$.**

$\{\mathcal{DBA}\ \ Set\}$	Cr_{i1}	Cr_{i2}	Cr_{i3}	Cr_{i4}	Cr_{i5}	Cr_{i6}
Cr_{1j}	$\{\mathcal{B}\zeta_1, \mathcal{B}\zeta_2, \mathcal{B}\zeta_3\}$	$\{\mathcal{B}\zeta_3\}$	$\{\mathcal{B}\zeta_1, \mathcal{B}\zeta_3\}$	$\{\mathcal{B}\zeta_3\}$	$\{\mathcal{B}\zeta_3\}$	$\{\mathcal{B}\zeta_2\}$
Cr_{2j}	$\{\mathcal{B}\zeta_3\}$	$\{\mathcal{B}\zeta_3, \mathcal{B}\zeta_5, \mathcal{B}\zeta_6\}$	$\{\mathcal{B}\zeta_3, \mathcal{B}\zeta_6\}$	$\{\mathcal{B}\zeta_3, \mathcal{B}\zeta_5, \mathcal{B}\zeta_6\}$	$\{\mathcal{B}\zeta_3, \mathcal{B}\zeta_5\}$	$\{\mathcal{B}\zeta_5\}$
Cr_{3j}	$\{\mathcal{B}\zeta_1, \mathcal{B}\zeta_3\}$	$\{\mathcal{B}\zeta_3, \mathcal{B}\zeta_6\}$	$\{\mathcal{B}\zeta_1, \mathcal{B}\zeta_3, \mathcal{B}\zeta_4, \mathcal{B}\zeta_6\}$	$\{\mathcal{B}\zeta_3, \mathcal{B}\zeta_6\}$	$\{\mathcal{B}\zeta_3\}$	$\{\}$
Cr_{4j}	$\{\mathcal{B}\zeta_3\}$	$\{\mathcal{B}\zeta_3, \mathcal{B}\zeta_5, \mathcal{B}\zeta_6\}$	$\{\mathcal{B}\zeta_3, \mathcal{B}\zeta_6\}$	$\{\mathcal{B}\zeta_3, \mathcal{B}\zeta_5, \mathcal{B}\zeta_6\}$	$\{\mathcal{B}\zeta_3, \mathcal{B}\zeta_5\}$	$\{\mathcal{B}\zeta_5\}$
Cr_{5j}	$\{\mathcal{B}\zeta_3\}$	$\{\mathcal{B}\zeta_3, \mathcal{B}\zeta_5\}$	$\{\mathcal{B}\zeta_3\}$	$\{\mathcal{B}\zeta_3, \mathcal{B}\zeta_5\}$	$\{\mathcal{B}\zeta_3, \mathcal{B}\zeta_5 6\}$	$\{\mathcal{B}\zeta_5\}$
Cr_{6j}	$\{\mathcal{B}\zeta_2\}$	$\{\mathcal{B}\zeta_5\}$	$\{\}$	$\{\mathcal{B}\zeta_5\}$	$\{\mathcal{B}\zeta_5\}$	$\{\mathcal{B}\zeta_2, \mathcal{B}\zeta_5\}$

$\mathcal{S}oS_5(\upsilon_{52}) = \{\mathcal{B}\zeta_3, \mathcal{B}\zeta_5\};$
$\mathcal{S}oS_6(\upsilon_{62}) = \{\mathcal{B}\zeta_2, \mathcal{B}\zeta_5\};$
$\mathcal{S}oS_6(\upsilon_{62}) = \{\mathcal{B}\zeta_1, \mathcal{B}\zeta_3, \mathcal{B}\zeta_5, \mathcal{B}\zeta_6\};$

To verify the applicability of bijective soft set to our problem, we consider (SoS_1, BA_1) as an example. We observe that union of all the soft sets of (SoS, BA_1) symbolizes concept sources, which is universal set U or $\bigcup_{\upsilon_{ij} \in BA_i} SoS(\upsilon_{1j}) = U$. Furthermore, if we consider any of two BA values, $\upsilon_{11}, \upsilon_{12} \in BA_1$, $\upsilon_{11} \neq \upsilon_{12}$, $SoS_1(\upsilon_{11}) \bigcap SoS_1(\upsilon_{12}) = \varnothing$.

iv We postulate our desired debris from building attributes as per 4, and denote it as DBA.

$[\mathcal{DBA}] = \{Foundations, Exterior\ \ walls, Floor, Structure, Interior\ \ partition, Verticle\ \ systems\}$

We consider two debris scenarios i.e., normal and the worst case to have better understandings of coverage using Wi-Fi signals given below.

Worst-debris case : $[\mathcal{DBA}_1] = \{Weak, Load\ bearing, Heavy\,weight, Weak, Heavy, Weak\}$

Normal debris case:$[\mathcal{DBA}_2] = \{Strong, Non\ load - bearing, Light\ weight, Strong, Light, Strong\}$

Then corresponding representation would be as follows;

$[\mathcal{DBA}_1] = \{\upsilon_{12}, \upsilon_{21}, \upsilon_{31}, \upsilon_{42}, \upsilon_{51}, \upsilon_{62}\}$
$[\mathcal{DBA}_2] = \{\upsilon_{11}, \upsilon_{22}, \upsilon_{32}, \upsilon_{41}, \upsilon_{52}, \upsilon_{61}\}$

Moreover, bijective soft sets for each required building attribute value as per postulates from $\mathcal{DBA}_1$ are as under;

$SoS(\upsilon_{12}) = \{\mathcal{B}\zeta_4, \mathcal{B}\zeta_5, \mathcal{B}\zeta_6\};$
$SoS(\upsilon_{21}) = \{\mathcal{B}\zeta_1, \mathcal{B}\zeta_2, \mathcal{B}\zeta_4\};$
$SoS(\upsilon_{31}) = \{\mathcal{B}\zeta_2, \mathcal{B}\zeta_5\};$
$SoS(\upsilon_{42}) = \{\mathcal{B}\zeta_1, \mathcal{B}\zeta_2, \mathcal{B}\zeta_4\};$
$SoS(\upsilon_{51}) = \{\mathcal{B}\zeta_1, \mathcal{B}\zeta_2, \mathcal{B}\zeta_4, \mathcal{B}\zeta_6\};$
$SoS(\upsilon_{62}) = \{\mathcal{B}\zeta_1, \mathcal{B}\zeta_3, \mathcal{B}\zeta_4, \mathcal{B}\zeta_6\};$

Similarly, bijective soft sets for $\mathcal{DBA}_2$ are;

$SoS(\upsilon_{11}) = \{\mathcal{B}\zeta_1, \mathcal{B}\zeta_2, \mathcal{B}\zeta_3\};$
$SoS(\upsilon_{22}) = \{\mathcal{B}\zeta_3, \mathcal{B}\zeta_5, \mathcal{B}\zeta_6\};$
$SoS(\upsilon_{32}) = \{\mathcal{B}\zeta_1, \mathcal{B}\zeta_3, \mathcal{B}\zeta_4, \mathcal{B}\zeta_6\};$
$SoS(\upsilon_{41}) = \{\mathcal{B}\zeta_3, \mathcal{B}\zeta_5, \mathcal{B}\zeta_6\};$
$SoS(\upsilon_{52}) = \{\mathcal{B}\zeta_3, \mathcal{B}\zeta_5\};$
$SoS(\upsilon_{61}) = \{\mathcal{B}\zeta_2, \mathcal{B}\zeta_5\};$

v We construct correlation tables from bijective soft sets using *AND* operation for both $\mathcal{DBA}_1$ and $\mathcal{DBA}_2$

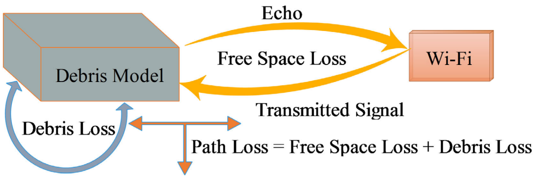

(a) Path Loss in Collapsed structure

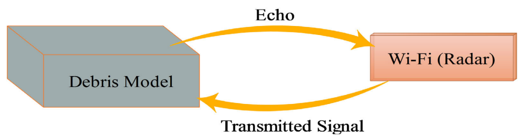

(b) Wi-Fi Radar

FIGURE 6. Illustration of coverage range methods.

TABLE 5. R-Union on Table 2.

	$R-Union$
$\bigcup_{i=1\to 6} Cr_{1j}$	$\{\mathcal{B}\zeta_4, \mathcal{B}\zeta_5, \mathcal{B}\zeta_6\}$
$\bigcup_{i=1\to 6} Cr_{2j}$	$\{\mathcal{B}\zeta_1, \mathcal{B}\zeta_2, \mathcal{B}\zeta_4\}$
$\bigcup_{i=1\to 6} Cr_{3j}$	$\{\mathcal{B}\zeta_2, \mathcal{B}\zeta_5\}$
$\bigcup_{i=1\to 6} Cr_{4j}$	$\{\mathcal{B}\zeta_1, \mathcal{B}\zeta_2, \mathcal{B}\zeta_4\}$
$\bigcup_{i=1\to 6} Cr_{5j}$	$\{\mathcal{B}\zeta_1, \mathcal{B}\zeta_2, \mathcal{B}\zeta_4, \mathcal{B}\zeta_6\}$
$\bigcup_{i=1\to 6} Cr_{6j}$	$\{\mathcal{B}\zeta_1, \mathcal{B}\zeta_3, \mathcal{B}\zeta_4, \mathcal{B}\zeta_6\}$

TABLE 6. R-Union on Table 4.

	$R-Union$
$\bigcup_{i=1\to 6} Cr_{1j}$	$\{\mathcal{B}\zeta_1, \mathcal{B}\zeta_2, \mathcal{B}\zeta_3\}$
$\bigcup_{i=1\to 6} Cr_{2j}$	$\{\mathcal{B}\zeta_3, \mathcal{B}\zeta_5, \mathcal{B}\zeta_6\}$
$\bigcup_{i=1\to 6} Cr_{3j}$	$\{\mathcal{B}\zeta_1, \mathcal{B}\zeta_3, \mathcal{B}\zeta_4, \mathcal{B}\zeta_6\}$
$\bigcup_{i=1\to 6} Cr_{4j}$	$\{\mathcal{B}\zeta_3, \mathcal{B}\zeta_5, \mathcal{B}\zeta_6\}$
$\bigcup_{i=1\to 6} Cr_{5j}$	$\{\mathcal{B}\zeta_3, \mathcal{B}\zeta_5\}$
$\bigcup_{i=1\to 6} Cr_{6j}$	$\{\mathcal{B}\zeta_2, \mathcal{B}\zeta_5\}$

according to rule 5. This operation is presented in Tables 1, 2, 3, and 4.

vi Furthermore, we apply R-Union on Tables 2 and 4 for both $\mathcal{DBA}_1$ and $\mathcal{DBA}_2$ as per 6 and show the results in Tables 5 and 6.

vii We perform intersection operation on Tables 5 and 6, but figure out that union correlation tables can not be reduced to 1×1. Therefore, we look into rules 5 and 6 for the most occuring concepts across $\mathcal{DBA}_1$ and $\mathcal{DBA}_2$ respectively. It will yield $\mathcal{B}\zeta_4$ as the most relevant building concept for $\mathcal{DBA}_1$, which is provided below;

$[\mathcal{DBA}] = \{Foundations, Exterior\ \ walls, Floor, Structure, Interior\ \ partition, Verticle\ \ systems\}$

$\mathcal{B}\zeta_4 = \{\upsilon_{12}, \upsilon_{21}, \upsilon_{32}, \upsilon_{42}, \upsilon_{51}, \upsilon_{62}\}$

This $\mathcal{B}\zeta_4$ corresponds to;

$\mathcal{B}\zeta_4 = \{Weak, Load\ bearing, Light\ weight, Weak, Heavy, Weak\}$

We also get $\mathcal{B}\zeta_1$, and $\mathcal{B}\zeta_4$ as second most favourable options for $\mathcal{DBA}_1$. Similarly, corresponding building concept for $\mathcal{DBA}_2$ is as follows;

$\mathcal{B}\zeta_3 = \{\upsilon_{11}, \upsilon_{22}, \upsilon_{32}, \upsilon_{41}, \upsilon_{52}, \upsilon_{62}\}$

$\mathcal{B}\zeta_3 = \{Strong, Non\ load-bearing, Light\ weight, Strong, Light, Weak\}$

Quite similar to $\mathcal{DBA}_2$, we also get other possible concept which is $\mathcal{B}\zeta_5$. However, we have to select only the most occuring concepts. So, $\mathcal{B}\zeta_4$ and $\mathcal{B}\zeta_3$ are the most suitable debris selection concepts for worst and normal scenarios.

Finally, let us analyze attained functional building concepts that may provide us proper insight towards better debris cases. As a conclusion, we figure out that weak foundations, load-bearing exterior building walls, lightweight floor, irrespective of structure type and interior partitions, and weak vertical systems result in such debris that can be subject to Wi-Fi signal penetration. This outcome has provided us trustworthiness in debris selection for better coverage. Afterward, we can apply the Wi-Fi radar technique to study the construction materials and verify the bijective soft set debris selection through proper simulations.

V. Wi-Fi RADAR METHOD

This section presents the Wi-Fi signal modeling on the selected debris in the preceding section. Firstly, we discuss the geometry and debris attenuations in the context of Wi-Fi signals. Afterward, we employ the Wi-Fi radar approach to study the coverage to verify the debris concept selection.

A. PROBLEM GEOMETRY

We consider echo models for both brick and masonry block as presented in Fig 4c and 4d to analyze the coverage of Wi-Fi radar signals. It is observed that Wi-Fi transmitters typically send signals in all directions. However, to model collapsed structures, we assume that the antenna points to the debris pattern to avoid unwanted resource reflections and treat them as noise. We also assume to place a Wi-Fi device outside the debris, with no other radio equipment nearby. These assumptions minimize the loss encountered to Wi-Fi signal path and comprise of two parts, as shown in Fig 6a, which are debris and free-space paths. Although these assumptions are strict, however, considering the nature and impact of collapsed structures for rescue and weak strength of Wi-Fi signals, we need to have these pre-conditions. If there are other radio devices in the vicinity, these will add interference and noises to CSI and can reduce detection. Moreover, wireless signals have to travel almost 1 meter in free space as a Wi-Fi device is placed outside of the rubble. Afterward, no sooner, the signal penetrates debris; it faces many decays, fading, attenuations, and damping from the noisy environment within the debris model. We map the Wi-Fi signals in debris through a simplified model in Fig 6a; and mathematically, it can be given as follows;

$$Path\,Loss = Loss_{free-space} + Loss_{debris} \tag{1}$$

B. DEBRIS SIGNAL LOSS

Let us analyze the (1) that encompasses all the losses encountered to the Wi-Fi signal in our debris model. As far as free-space loss is concerned, we deal with it separately while presenting the Wi-Fi radar method. However, debris losses need proper attention because Wi-Fi signals can even completely damp due to higher scattering, reflections, diffractions, and fading. We observe that wireless signal face both slow and fast fading, but that study is out of the scope of this work due to the complex nature of debris where traditional fading and scattering does not work well, and there is need to redefine those statistical models in the context of collapsed structures. Therefore, we merely exploit the attenuations factors values from existing literature and introduce them to our debris problem, because this itself is a big contribution as it provides better insight about debris selection. We denote attenuations as X_G and provide a relation on attenuation based losses as follows;

$$\begin{aligned} Loss_{debris} &= X_G = Attenuations(Structural\ layers) \\ &\quad + Attenuations(Non-structural\ layers) \end{aligned} \tag{2}$$

$$\begin{aligned} Loss_{debris} &= X_G = a * AF(Br\ or\ Blk) + b * AF(Con) \\ &\quad + c * AF(Gls) + d * AF(Lum) + e * AF(Dbr) \end{aligned} \tag{3}$$

where a, b, c, d, and e represents the number of layers for both structural and non-structural materials as indicated in (2) and shown in Fig 4. Moreover, AF is an attenuation factor caused by a single layer of these materials, and it alters with their thickness level correspondingly.

C. Wi-Fi RADAR

Let us discuss the Wi-Fi radar method to study the debris selection, as shown in Fig 6b. This approach follows the principle of Doppler radar, where pulses are transmitted after a particular interval. These signals strike with each object on their way and reflect towards the receiver. This approach is quite different than a normal transmitter-receiver (TR) approach [31]. We observe that all existing Wi-Fi sensing applications comply with the TR method and do not consider the radar range technique. The very reason to use TR in those applications is problem geometry and scope. However, we cannot employ the same method in debris scenario as the receiver is assumed to be outside of rubble. So, the only way is to address coverage; is by employing radar range technique, where reflections having desired breathing information encompassed in CSI. To the best of our knowledge, there is no proper study that deals with Wi-Fi radar with debris selection. Although there is work by authors [33], where we focused on Wi-Fi signals more rather than debris selection. So, this study is much needed to have better understandings of debris in the context of Wi-Fi radar.

To formulate Wi-Fi radar, we revisit our building assessment and echo model, as discussed in Section II-C. This Wi-Fi radar depends on the cross-sectional area (debris in our case), signal intensities, antenna gains and distance between object and transmitter, given as below;

$$P_r = P_t G_t G_r \left(\frac{c^2 \sigma}{(4\pi)^3 f^2 R^4}\right) \tag{4}$$

where P_t,P_r, G_t, and G_r symbolizes power and gains of Wi-Fi radar transceiver. σ is cross-sectional area, which we consider as debris area while f and R implies to frequency and range correspondingly. Afterward, by employing [33], we get received signal as;

$$\left\{\begin{matrix} WiFi\ Signal\ received \\ at\ WiFi\ Radar \end{matrix}\right\} = \frac{P_t G_t \lambda^2 4\pi\sigma}{(4\pi R)^2 \lambda^2} \times \frac{G_r \lambda^2}{(4\pi R)^2} \tag{5}$$

We can reduce (5) to log form as follows;

$$P_R = G_T + G_R + G_\sigma + P_T - 2\beta_1 \tag{6}$$

Here, β_1 is free-space loss encountered to Wi-Fi radar signals as we discussed in (1), whereas G_σ represents target gain factor. Afterward, we integrate debris losses from (2) in (6), and reconvert log form to normal scale to get final coverage in debris, given as below;

$$WiFiRadar\ Range = R = \sqrt[4]{\frac{P_t G_t G_r}{P_r}\left(\frac{\lambda^2 \sigma}{(4\pi)^3}\right)\frac{1}{X_g}} \tag{7}$$

D. CSI CONSIDERATION FOR Wi-Fi RADAR

Wi-Fi signals have a feature known as CSI that encompasses information of desired events happening within the channel. It has led to all novel Wi-Fi sensing applications. As we aim to investigate debris concept selection for Wi-Fi radar, it is a must for an echo signal to comply with CSI for breathing detection. This echo contains noises and clutter in CSI, which can lead to untrustworthy breathing detection. Therefore, we need to have such an echo signal that has the desired CSI. We envisage that signal to noise ratio (SNR) of received signal P_r in (7) should be above or equal to PDT as $SNR \geq SNR_T$.

VI. NUMERICAL RESULTS

In this section, we discuss our simulation method for debris concept selection and evaluate results.

A. METHOD

To obtain substantive results, we precisely select the simulation parameters, as shown in Table 7. We simulate debris cases in MATLAB 18a.

Now, let's discuss the motivation for selecting these simulation parameters. We study two operating frequencies of Wi-Fi Halow, i-e., China (779MHz) and the US (902MHz),

TABLE 7. Simulation parameters.

Parameter	Values
Operational Frequencies Transmission Power Antenna Gains	(902, 779)MHz (23, 13, 10) dBm (13, 23, 26) dBi
Radar Cross Section Materials(Structural) Materials(Non-structural)	$4m^2$ Brick 10.5″, Concrete 8″ Masonary Block 12″, Masonary Block 16″ Glass 0.5″, Lumber 3″, Brick 3.5″
Attenuations values	Concrete 8″= c = 23dB Masonary Block 12″= bl = 14dB Masonary Block 16″= bl = 17dB Glass 0.5″= g = 2dB Lumber 3″= l = 2.8dB Brick 3.5″= db = 3.5dB
Brick based debris cases	D1 = 10 (3b+2c+2g+2l+db) D2 = 15 (6b+2c+2g+3l+2db) D3 = 23 (10b+3c+2g+5l+3db) D4 = 30 (13b+4c+3g+6l+4db)
Masonary block (12″, 16″) based debris cases	D1 = 10 (3bl+2c+2g+2l+db) D2 = 14 (5bl+2c+2g+3l+2db) D3 = 20 (7bl+3c+2g+5l+3db) D4 = 26 (9bl+4c+3g+6l+4db)
Modulation Type Channel Bandwidth Signal PTD	256QAM, 64QAM, 16QAM 1MHz at 256QAM 1MHz at 64QAM 1MHz at 16QAM -70dBm at 256QAM -77dBm at 64QAM -71dBm at 16QAM

as given in [34], [44], [45] to realize our field surveys into theory and global endorsement. These frequencies are regulated by IEEE Task Group [44], and have their signal intensities and antenna consideration for the Wi-Fi Halow spectrum. Furthermore, the inverse relationship between power and antenna is regulated by the Federal Communications Commission (FCC)[9] para 17.245 rules for Point to multipoint (PTMP).[10]

[9]https://www.fcc.gov/tags/radio-rules
[10]https://www.air802.com/fcc-rules-and-regulations.html

Next, we consider the reasons for debris materials, nature, layers, and attenuations. We classify building debris into structural (concrete, brick, and masonry block) and non-structural (glass, lumber, and décor brick) materials with thickness level, as shown in Table 7, which is carefully taken after field surveys. Now, let's consider masonry block, it is the primary source of wall construction in Balakot field site, and two thickness standards are used in that area. Similarly, brick refers to the Wenchuan site. Furthermore, all these structural and non-structural materials have their attenuation factor for a single layer, which we employed from Digi[11] and U.S. National Institute of Standards and Technology(NIST).[12] Moreover, we consider four different debris layered cases starting from low to high complexity for both brick and block cases. This brick and block classification is only limited to walls, whereas other materials are the same.

Finally, we discuss the Wi-Fi Halow signal communication parameters. We select these values by looking into signal PTD from [34], [44], [45] for three QAM types (256, 64, 16) with 1MHz channel bandwidth as it can ensure better CSI. Higher QAM ensures a better data rate but is subject to interference and noise. Therefore, we consider both low and high for a proper comparison of Wi-Fi signals in debris cases.

B. RESULTS

We simulated the debris cases for criteria as discussed earlier for better debris concept selection and show results in Table 8 and 9. These results present Wi-Fi Halow coverage for four debris cases at varying signal intensities across frequencies, antenna gains, and modulation schemes. We test these parameters through various combinations for 144 times to have a proper comparison for debris. Moreover, we compare the simulation results in succeeding sections.

[11]http://ftp1.digi.com/support/images/XST-AN005a-IndoorPathLoss.pdf
[12]http://www.eiwellspring.org/shielding.html

TABLE 8. Debris study at 902MHz.

Transmit Power dBm	Max Antenna dBi	Range in Collapsed Structure (m)											
		Brick type				Masonary block type 1				Masonary block type 2			
		D 1	D 2	D 3	D 4	D 1	D 2	D 3	D 4	D 1	D 2	D 3	D 4
		QAM 256(R =5/6)(MS=-70dBm)											
23 13 10	13 23 26	8.1058 14.4143 17.1315	1.6838 2.9943 3.5587	0.0529 0.0941 0.1119	0.0026 0.0046 0.0055	2.4199 4.3032 5.1144	0.3360 0.5974 0.7101	0.0106 0.0188 0.0223	3.477e-4 6.184e-4 7.351e-4	1.4414 2.5633 3.0465	0.1417 0.2519 0.2994	0.0032 0.0056 0.0067	7.350e-5 1.307e-4 1.553e-4
		QAM 16(R =3/4)(MS=-71dBm)											
23	13	8.5861	1.7836	0.0561	0.0028	2.4199	0.3360	0.0106	3.477e-4	1.4414	0.1417	0.0032	7.350e-5
		QAM 64(R =5/6)(MS=-77dBm)											
13 10	23 26	21.5672 25.6327	4.4802 5.3247	0.1409 0.1674	0.0069 0.0082	4.3032 5.1144	0.5974 0.7101	0.0188 0.0223	6.184e-4 7.350e-4	2.5619 3.0465	0.2519 0.2994	0.0056 0.0067	1.307e-4 1.553e-4

TABLE 9. Debris study at 779MHz.

Transmit Power dBm	Max Antenna dBi	Range in Collapsed Structure (m)											
		Brick type				Masonary block type 1				Masonary block type 2			
		D 1	D 2	D 3	D 4	D 1	D 2	D 3	D 4	D 1	D 2	D 3	D 4
		QAM 256(R =5/6)(MS=-70dBm)											
23	13	8.7223	1.8119	0.0570	0.0028	2.6039	0.3615	0.0114	3.742e-4	1.5511	0.1525	0.0034	7.909e-5
13	23	15.5106	3.2220	0.1013	0.0050	4.6305	0.6429	0.0202	6.657e-4	2.7582	0.2711	0.0060	1.407e-4
10	26	18.4344	3.8294	0.1204	0.0059	5.5034	0.7641	0.0240	7.909e-4	3.2781	0.3222	0.0072	1.672e-4
		QAM 16(R =3/4)(MS=-71dBm)											
23	13	9.2391	1.9192	0.0603	0.0030	2.6039	0.3615	0.0114	3.742e-4	1.5511	0.1525	0.0034	7.909e-5
		QAM 64(R =5/6)(MS=-77dBm)											
13	23	23.2075	4.8209	0.1516	0.0075	4.6305	0.6429	0.0202	6.655e-4	2.7582	0.2711	0.0060	1.407e-4
10	26	27.5822	5.7297	0.1801	0.0089	5.5034	0.7641	0.0240	7.909e-4	3.2781	0.3222	0.0072	1.672e-4

1) COVERAGE W.R.T ALL DEBRIS CASES

We discussed in preceding sections to classify debris into four cases from low to high complexity level. Now, let us study the coverage in these multilayered scenarios of brick and masonry blocks.

Firstly, we consider the simulations results for all debris cases of 902MHz as an example from Table 8 and plot them as individual value plot in Fig 7. We observe that at lower debris D1 with masonry block type 1 for 23dBm of power with QAM (256 and 16), we get the almost same coverage of 2.42m, whereas, with the same parameter for D4, the coverage is 0.001m. Similarly, for masonry block type 2 with D1, the coverage is 1.442m, and for D4, it is 0.001m, respectively. Likewise, coverage for brick debris D1 for the same parameters is 8.587m and 8.106m for D1 and 0.003m, each correspondingly. This shows an increasing trend of coverage with less thick debris case. Furthermore, if we consider low power, i.e., 10dBm, the coverage for block type 1 is 5.115m at D1 and 0.001m at D4 and for block type 2; it is D1 = 3.047m and D4 = 0.001m, and finally brick has coverage D1 = (17.132m,25.633m) and D4 = (0.006m,0.009m) correspondingly. This behavior shows that low power with low thickness debris materials provides better coverage while employing the Wi-Fi radar method. We find a similar trend for 779MHz frequency, as plotted in Fig 8. By comparing Fig 7, and 8, we figure out that brick-based wall construction is the most feasible debris for Wi-Fi signals, whereas masonry blocks provide very weak coverage.

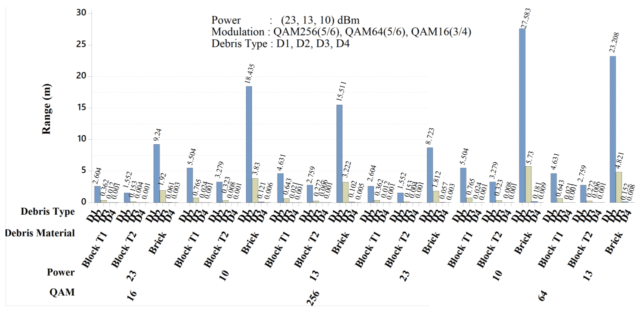

FIGURE 8. Range with all debris cases (779 MHz).

2) COVERAGE W.R.T LOW LAYERED DEBRIS CASES

Let us have a more detailed comparison with respect to low layered debris cases because from section VI-B.1, we observe that Wi-Fi signals yield better results at fewer rubble scenarios. We plot low layered debris cases for both 902MHz and 779MHz in Fig 9 and 10, and find a similar coverage trend. These plots give a more detailed view of debris behavior.

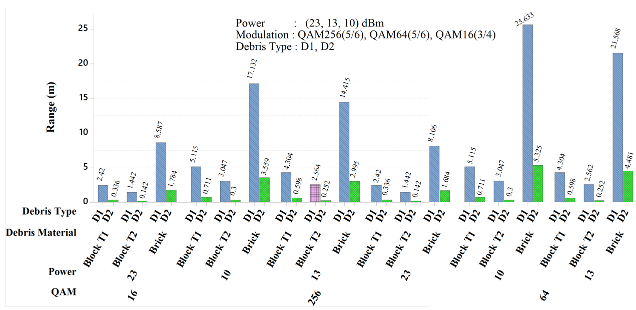

FIGURE 9. Low layered debris cases (902 MHz).

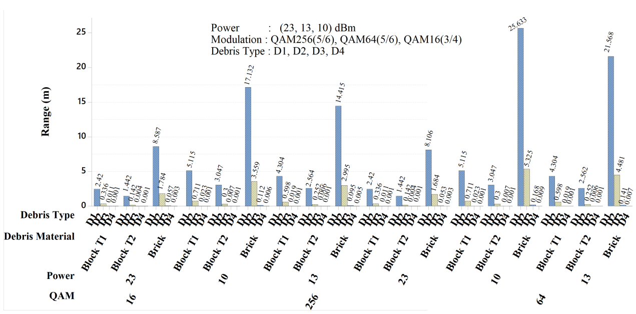

FIGURE 7. Range with all debris cases (902 MHz).

Now, let us consider Fig 10 as an example, the coverage at D1 with masonry block type 1 with 23dBm of power QAM

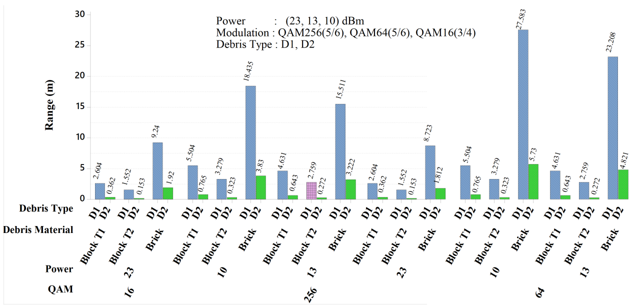

FIGURE 10. Low layered debris cases (779 MHz).

(256 and 16) is 2.604m, whereas, with the same parameter for D2, the coverage is 0.362m. Similarly, for masonry block type 2 with D1, the coverage is 1.552m, and for D2, it is 0.153m, respectively. Likewise, coverage for brick debris D1 for the same parameters is 9.24m and 8.72m for D1 and 1.92m and 1.8812m correspondingly. This trend is similar to one in VI-B.1, where we observe better coverage with fewer debris layers. Furthermore, if we consider low power, i.e., 10dBm, the coverage for block type 1 is D1 = 5.504m and D2 = 0.765m, and for block type 2; it is D1 = 3.279m and D2 = 0.323m, and finally brick has coverage D1 = (18.435m,27.583) and D2 = (3.83 m,5.73m) correspondingly. From this comparison, we again conclude that low power yields better coverage, and brick debris is the most suited construction.

3) COVERAGE W.R.T HEAVY LAYERED DEBRIS CASES

Now, let us further investigate the Wi-Fi Halow signal coverage at higher debris to have deep analysis. We plotted simulation results for heavy layered debris as individual value plot for both frequencies in Fig 11 and 12, respectively. We consider Fig 12 for comparison and analysis. The coverage at 10dBm across respective QAMs for block type 1 is 0.012m at D3 and 0.001m at D4 and for block type 2; it is D3 = 0.004m and D4 = 0.0001m, and finally brick has coverage D3 = (0.061m,0.057m) and D4 = 0.003 each correspondingly.

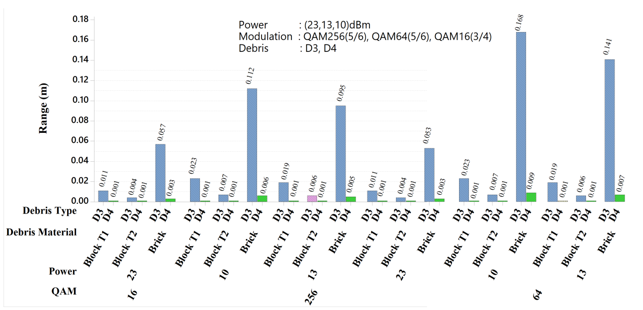

FIGURE 11. Heavy layered debris cases (902 MHz).

This trend is similar to one in VI-B.2; but, here we observe weak coverage due to heavy debris layers. Furthermore, if we consider low power, i.e., 10dBm, the coverage for block type 1 is 0.024m at D3 and 0.001m at D4 and for block type 2; it is D3 = 0.008m and D4 = 0.001m, and finally brick has coverage D3 = (0.121m, 0.181m) and D4 = (0.006m,0.009m) respectively. Therefore, we observe a similar trend to VI-B.2, whereby lowing the power, the coverage is increased.

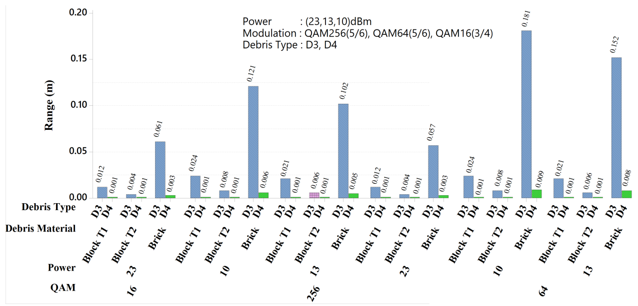

FIGURE 12. Heavy layered debris cases (779 MHz).

4) FREQUENCY-WISE COVERAGE COMPARISON

Finally, we compare the debris cases for Wi-Fi Halow frequencies. We classify it as a deeply layered and heavy layered comparison, as shown in Fig 13 and 14, respectively. Here, we denote frequencies with F1 = 779MHz and F2 = 902MHz. Now, let us consider only one case, i.e., Fig 13 as an example because all others follow a similar trend as discussed in prior sections. Here, 256 (a,b,c) represents corresponding power which is 23dBm, 13dBm and 10dBm correspondingly.

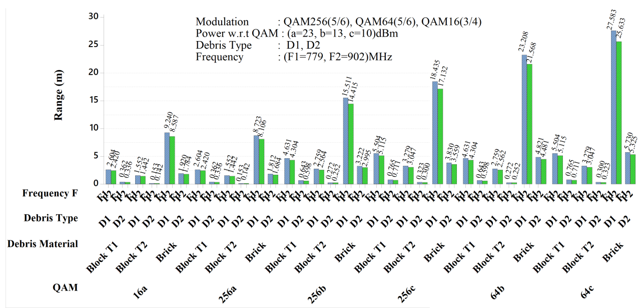

FIGURE 13. Frequency wise low layered debris cases.

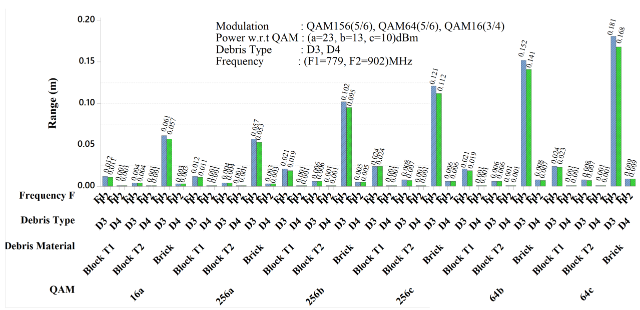

FIGURE 14. Frequency wise heavy layered debris cases.

Now, to simplify the comparison, we only consider just a brick case at lower power, i.e., 10dBm for respective

QAMs. Here, the coverage of brick at D1 is (F1 = 9.240m, F2 = 8.587m) for QAM16, and it is (F1 = 8.723m, F2 = 8.106m) respectively. Similarly, the with same parameters, the coverage at D2 is (F1 = 1.920m, F2 = 1.784m) and (F1 = 1.812m, F2 = 1.684m), correspondingly. From this comparison, we observe an increasing trend of coverage while lowering the frequency. In conclusion, from the above sections, we find that low frequency with less brick debris can be an effective debris selection mechanism for Wi-Fi radar.

VII. PERFORMANCE ANALYSIS

In this section, we analyze our work. Firstly, we discuss the idea of debris selection in the context of Wi-Fi radar signals from existing literature. Afterward, we examine the bijective soft set and Wi-Fi radar techniques for debris cases. Finally, we discuss the significance, applications, insinuations, and limitations of this work.

Let us discuss the need to study the debris information analysis for Wi-Fi radar edge in collapsed structures. Authors in their previous work [30]–[33] pointed out that Wi-Fi signals can be used to address coverage in collapsed structures. However, the strength of these Wi-Fi signals is weak, owing to multi-layered debris, attenuations, noises, and clutters. Therefore, in this study, we investigate multi-layered debris in particular. To achieve our goal, we narrowed down the disaster scenarios to earthquakes and modeled the debris for proper evaluation. The motivation behind employing Wi-Fi signals to collapsed structures is the non-existence of any successful post-disaster rescue solutions in spite of the IoT era. Although, there are some rescue techniques, as discussed in Section I-A. However, those methods are expensive and cannot be deployed in developing countries. Howsoever, Wi-Fi sensing applications provide insight for possible cost-effective rescue solutions, but coverage is a big challenge, as addressed above.

Now, let us analyze the methods for debris analysis. We conducted field surveys of earthquake sites from China and Pakistan and investigated the causes of structural collapses. Based on this investigation, we developed the collapsed building assessment, debris, and echo models to map field surveys into theory. After that, we employed the bijective soft set technique introduced by Tiwari in [35] for a multi-attribute decision-making problem in the engineering domain. We applied this method and selected the best and worst cases for debris, which are then subject to Wi-Fi radar [33] signal coverage. Moreover, we address CSI for Wi-Fi radar echo, as this is the main parameter to employ breathing detection techniques for possible rescue.

Furthermore, we verify the methods for debris concept selection. Our bijective soft set approach in Section IV provides us the debris cases which are most suitable for Wi-Fi signals. These scenarios are building functional concepts $\mathcal{B}\zeta_3$ and $\mathcal{B}\zeta_4$ respectively. We conclude that weak foundations, loadbearing exterior building walls, lightweight floor, irrespective of structure type and interior partitions, and weak vertical systems yield the most relevant debris. Similarly, results of Wi-Fi radar method in Section VI also ensures that less debris case verify the $\mathcal{B}\zeta_3$ and $\mathcal{B}\zeta_4$. Therefore, we figure out that buildings with brick-based load-bearing walls along with other structural and non-structural materials for lightweight floor and interior partitions can be the most suitable debris for Wi-Fi radar coverage in collapsed environments.

Finally, we discuss the prospects of this work. We observe that this debris study provides reasonably better insight into Wi-Fi signals. As discussed in Section I-A, that Wi-Fi sensing application for breathing detection in [18] along-with [15] can be employed for rescue in collapsed structures. Therefore, this study fills one gap in proper debris analysis. Further investigation on multipath fading, attenuations, and damping will lead to better Wi-Fi signal strength. Moreover, we have used Wi-Fi Halow for our debris investigation, which is a low power standard primarily designed for IoTs. Due to this, we may envisage having IoT based rescue solutions in the future.

A. LIMITATIONS

Like any other research study, this work also has some limitations. The first and the most significant is the lack of practical implementation of the Wi-Fi radar method to field surveys as we confined ourselves only to simulations. However, this is due to the primitive nature of this work, and we need to perform simulations before having any practical deployments. Howsoever, we do have practical field surveys and developed collapsed building assessments and debris models. And, we also verify effectiveness through a bijective soft set approach, which provides insight into the nature of debris feasible for Wi-Fi under these standard conditions. Similarly, we employed the attenuation factor loss model for Wi-Fi radar, which may not be much feasible due to fading, scattering, noises, and clutter. However, we are certain to have better coverage as attenuation values of these materials have been practically estimated by Digi and NIST. The scope of this study was to investigate debris nature. Therefore, we only used existing practical deployment values rather than simulating fading that would yield only theoretical results. To practically deploy the Wi-Fi sensing solution, there is a need to have practical study on attenuations, losses, fading, and related phenomena. However, we are optimistic that this study will trigger further research to address multipath fading, scattering, or related challenges to increase the Wi-Fi signal strength.

VIII. CONCLUSION

In this paper, we studied the debris concept selection for effective coverage of Wi-Fi radar in collapsed structures. To accomplish our goal, we narrowed down disaster scenarios to an earthquake and then conducted field surveys for two different sites from two countries to better analyze the collapsed structures. We observed that it was much needed to investigate debris materials, collapsed types, and impact of Wi-Fi signals to these debris cases. Therefore, we used a bijective soft set technique from operational research to properly select debris cases and materials through various models. Afterward, we employed our Wi-Fi radar method to study the coverage of Wi-Fi Halow signals for the debris cases obtained from the bijective soft set technique. Finally, simulations results verified the coverage of Wi-Fi radar for less debris case with brick as feasible materials for wall bearing structures. Furthermore, we envision that proper study of attenuations and multipath fading is much needed to address the clutter and noises in debris.

REFERENCES

[1] P. Nurmi and S. Tarkoma, "Low-cost support for search and rescue operations using off-the-shelf sensor technologies," *Electron. Lett.*, vol. 53, no. 15, pp. 1011–1013, Jul. 2017.

[2] R. Huo *et al.*, "The trapped human experiment," *J. Breath Res.*, vol. 5, no. 4, Sep. 2011, Art. no. 046006.

[3] Y.-Y. Shih, A.-C. Pang, and P.-C. Hsiu, "A Doppler effect based framework for Wi-Fi signal tracking in search and rescue operations," *IEEE Trans. Veh. Technol.*, vol. 67, no. 5, pp. 3924–3936, May 2018.

[4] Z. Zhou, C. Wu, Z. Yang, and Y. Liu, "Sensorless sensing with WiFi," *Tsinghua Sci. Technol.*, vol. 20, no. 1, pp. 1–6, Feb. 2015.

[5] R. Poudel, Y. Hirai, M. Asari, and S.-I. Sakai, "Field study of disaster waste management and disposal status of debris after Gorkha Earthquake in Kathmandu, Nepal," *J. Mater. Cycles Waste Manage.*, vol. 21, no. 4, pp. 753–765, Feb. 2019.

[6] F. Niroui, K. Zhang, Z. Kashino, and G. Nejat, "Deep reinforcement learning robot for search and rescue applications: Exploration in unknown cluttered environments," *IEEE Robot. Autom. Lett.*, vol. 4, no. 2, pp. 610–617, Apr. 2019.

[7] X. Wang and X. Yang, "Structure design of a miniature and jumping robot for search and rescue," *J. Eng.*, vol. 2019, no. 13, pp. 219–224, Jan. 2019.

[8] L. Crocco and V. Ferrara, "A review on ground penetrating radar technology for the detection of buried or trapped victims," in *Proc. Int. Conf. Collaboration Technol. Syst. (CTS)*, May 2014, pp. 535–540.

[9] P. Agrafiotis, A. Doulamis, G. Athanasiou, and A. Amditis, "Real time earthquake's survivor detection using a miniaturized LWIR camera," in *Proc. 9th ACM Int. Conf. Pervasive Technol. Related Assistive Environ. (PETRA)*, 2016, pp. 21:1–21:4.

[10] J. Wang, Z. Cheng, L. Jing, and T. Yoshida, "Design of a 3D localization method for searching survivors after an earthquake based on WSN," in *Proc. 3rd Int. Conf. Awareness Sci. Technol. (iCAST)*, Sep. 2011, pp. 221–226.

[11] D. Zhang, S. Sessa, R. Kasai, S. Cosentino, C. Giacomo, Y. Mochida, H. Yamada, M. Guarnieri, and A. Takanishi, "Evaluation of a sensor system for detecting humans trapped under rubble: A pilot study," *Sensors*, vol. 18, no. 3, p. 852, Mar. 2018.

[12] Y. Sun, X. Wen, Z. Lu, T. Lei, and S. Jiang, "Localization of WiFi devices using unmanned aerial vehicles in search and rescue," in *Proc. IEEE/CIC Int. Conf. Commun. China*, Aug. 2018, pp. 147–152.

[13] T. Latif, E. Whitmire, T. Novak, and A. Bozkurt, "Sound localization sensors for search and rescue biobots," *IEEE Sensors J.*, vol. 16, no. 10, pp. 3444–3453, May 2016.

[14] M. Li, Y. Meng, J. Liu, H. Zhu, X. Liang, Y. Liu, and N. Ruan, "When CSI meets public WiFi: Inferring your mobile phone password via WiFi signals," in *Proc. ACM SIGSAC Conf. Comput. Commun. Secur. (CCS)*, 2016, pp. 1068–1079.

[15] L. Gui, M. Yang, H. Yu, J. Li, F. Shu, and F. Xiao, "A Cramér–Rao lower bound of CSI-based indoor localization," *IEEE Trans. Veh. Technol.*, vol. 67, no. 3, pp. 2814–2818, Mar. 2018.

[16] H. Wang, D. Zhang, Y. Wang, J. Ma, Y. Wang, and S. Li, "RT-Fall: A real-time and contactless fall detection system with commodity WiFi devices," *IEEE Trans. Mobile Comput.*, vol. 16, no. 2, pp. 511–526, Feb. 2017.

[17] J. Zhang, B. Wei, W. Hu, and S. S. Kanhere, "WiFi-ID: Human identification using WiFi signal," in *Proc. Int. Conf. Distrib. Comput. Sensor Syst. (DCOSS)*, May 2016, pp. 75–82.

[18] X. Liu, J. Cao, S. Tang, J. Wen, and P. Guo, "Contactless respiration monitoring via off-the-shelf WiFi devices," *IEEE Trans. Mobile Comput.*, vol. 15, no. 10, pp. 2466–2479, Oct. 2016.

[19] F. Li, C. Xu, Y. Liu, Y. Zhang, Z. Li, K. Sharif, and Y. Wang, "Mo-sleep: Unobtrusive sleep and movement monitoring via Wi-Fi signal," in *Proc. IEEE 35th Int. Perform. Comput. Commun. Conf. (IPCCC)*, Dec. 2016, pp. 1–8.

[20] H. Abdelnasser, M. Youssef, and K. A. Harras, "WiGest: A ubiquitous Wi-Fi-based gesture recognition system," in *Proc. IEEE Conf. Comput. Commun. (INFOCOM)*, Apr. 2015, pp. 1472–1480.

[21] G. Wang, Y. Zou, Z. Zhou, K. Wu, and L. M. Ni, "We can hear you with Wi-Fi!" in *Proc. 20th Annu. Int. Conf. Mobile Comput. Netw. (MobiCom)*, 2014, pp. 1–12.

[22] A. DiCarlofelice, E. DiGiampaolo, M. Feliziani, and P. Tognolatti, "Experimental characterization of electromagnetic propagation under rubble of a historic town after disaster," *IEEE Trans. Veh. Technol.*, vol. 64, no. 6, pp. 2288–2296, Jun. 2015.

[23] C. L. Holloway, G. Koepke, D. Camell, W. F. Young, and K. A. Remley, "Propagation measurements before, during, and after the collapse of three large public buildings," *IEEE Antennas Propag. Mag.*, vol. 56, no. 3, pp. 16–36, Jun. 2014.

[24] C. Phillips, D. Sicker, and D. Grunwald, "A survey of wireless path loss prediction and coverage mapping methods," *IEEE Commun. Surveys Tuts.*, vol. 15, no. 1, pp. 255–270, 1st Quart., 2013.

[25] S. Y. Seidel and T. S. Rappaport, "914 MHz path loss prediction models for indoor wireless communications in multifloored buildings," *IEEE Trans. Antennas Propag.*, vol. 40, no. 2, pp. 207–217, Feb. 1992.

[26] A. Aragón-Zavala, *Indoor Wireless Communications: From Theory to Implementation*. Hoboken, NJ, USA: Wiley, 2017. [Online]. Available: https://onlinelibrary.wiley.com/doi/book/10.1002/9781119004547

[27] M. Farin, V. C. Tsai, M. P. Lamb, and K. E. Allstadt, "A physical model of the high-frequency seismic signal generated by debris flows," *Earth Surf. Processes Landforms*, vol. 44, no. 13, pp. 2529–2543, Jul. 2019.

[28] Z. Shi, F. Wei, and V. Chandrasekar, "Radar-based quantitative precipitation estimation for the identification of debris flow occurrence over earthquake-affected regions in Sichuan, China," *Natural Hazards Earth Syst. Sci.*, vol. 18, no. 3, pp. 765–780, Mar. 2018.

[29] C. Zeng, P. Cui, Z. Su, Y. Lei, and R. Chen, "Failure modes of reinforced concrete columns of buildings under debris flow impact," *Landslides*, vol. 12, no. 3, pp. 561–571, Apr. 2014.

[30] M. F. Khan, G. Wang, M. Z. A. Bhuiyan, and X. Li, "Wi-Fi signal coverage distance estimation in collapsed structures," in *Proc. IEEE Int. Symp. Parallel Distrib. Process. Appl. (ISPA)*, Dec. 2017, pp. 1066–1073.

[31] M. F. Khan, G. Wang, and M. Z. A. Bhuiyan, "Wi-Fi frequency selection concept for effective coverage in collapsed structures," *Future Gener. Comput. Syst.*, vol. 97, pp. 409–424, Aug. 2019.

[32] M. F. Khan, G. Wang, M. Z. A. Bhuiyan, and T. Peng, "Wi-Fi Halow signal coverage estimation in collapsed structures," in *Proc. IEEE 16th Int. Conf. Dependable, Auton. Secure Comput. (DASC)*, Aug. 2018, pp. 626–633.

[33] M. F. Khan, G. Wang, M. Z. A. Bhuiyan, and X. Xing, "Towards Wi-Fi radar in collapsed structures," in *Proc. IEEE Ubiquitous Intell. Comput. (UIC)*, Oct. 2018, pp. 664–670.

[34] S. Aust, R. V. Prasad, and I. G. M. M. Niemegeers, "Outdoor long-range WLANs: A lesson for IEEE 802.11ah," *IEEE Commun. Surveys Tuts.*, vol. 17, no. 3, pp. 1761–1775, 3rd Quart., 2015.

[35] V. Tiwari, P. K. Jain, and P. Tandon, "A bijective soft set theoretic approach for concept selection in design process," *J. Eng. Des.*, vol. 28, no. 2, pp. 100–117, Jan. 2017.

[36] H. Yu, Y. Ma, L. Wang, Y. Zhai, and Z. Du, "A method for evaluating the rescue priority level of power line post-disaster based on AHP," in *Proc. IEEE Int. Conf. Mechatronics Automat. (ICMA)*, Aug. 2017, pp. 35–39.

[37] H. Inokuchi and T. Akiyama, "Debris treatment planning for large-scale earthquakes using fuzzy information," in *Proc. Joint 8th Int. Conf. Soft Comput. Intell. Syst. (SCIS) 17th Int. Symp. Adv. Intell. Syst. (ISIS)*, Aug. 2016, pp. 478–483.

[38] D. Molodtsov, "Soft set theory—First results," *Comput. Math. Appl.*, vol. 37, pp. 19–31, Feb. 1999.

[39] K. Gong, Z. Xiao, and X. Zhang, "The bijective soft set with its operations," *Comput. Math. Appl.*, vol. 60, no. 8, pp. 2270–2278, Oct. 2010.

[40] H. Khizar, M. I. Ali, J. C. R. Alcantud, B.-Y. Cao, and K. U. Tariq, "Best concept selection in design process: An application of generalized intuitionistic fuzzy soft sets," *J. Intell. Fuzzy Syst.*, vol. 35, no. 5, pp. 5707–5720, Nov. 2018.

[41] K. Hayat, M. I. Ali, F. Karaaslan, B.-Y. Cao, and M. H. Shah, "Design concept evaluation using soft sets based on acceptable and satisfactory levels: An integrated TOPSIS and Shannon entropy," *Soft Comput.*, to be published.

[42] V. Tiwari, P. K. Jain, and P. Tandon, "An integrated Shannon entropy and TOPSIS for product design concept evaluation based on bijective soft set," *J. Intell. Manuf.*, vol. 30, no. 4, pp. 1645–1658, Jul. 2017.

[43] M. I. Ali, F. Feng, X. Liu, W. K. Min, and M. Shabira, "On some new operations in soft set theory," *Comput. Math. Appl.*, vol. 57, no. 9, pp. 1547–1553, May 2009.

[44] *IEEE Standard for Information Technology—Telecommunications and Information Exchange Between Systems—Local and Metropolitan Area Networks—Specific Requirements—Part 11: Wireless LAN Medium Access Control (MAC) and Physical Layer (PHY) Specifications*, IEEE Standard 802.11-2007 (Revision IEEE Standard 802.11-1999), Jun. 2007, pp. 1–1238.

[45] *IEEE Draft Standard for Information Technology—Telecommunications and Information Exchange Between Systems—Local and Metropolitan Area Networks—Specific Requirements—Part 11: Wireless LAN Medium Access Control (MAC) and Physical Layer (PHY) Specifications: Amendment-Sub 1 GHz License-Exempt Operation*, IEEE Standard P802.11ah/D2.0, Apr. 2014, pp. 1–582.

MUHAMMAD FAIZAN KHAN received the B.Sc. degree in information and communication system engineering from the National University of Science and Technology, Pakistan, and the master of engineering degree in communication and information systems from the Huazhong University of Science and Technology, China. He is currently pursuing the Ph.D. degree in computer science with Guangzhou University, China. Earlier, he was a Lecturer with the University of South Asia, Pakistan. He has published articles in leading venues, such as FGCS, the IEEE ISPA, IEEE DASC, IEEE UIC, and IEEE ICUFN.

GUOJUN WANG was a Professor with Central South University, China; a Visiting Scholar with Temple University and Florida Atlantic University, USA; a Visiting Researcher with The University of Aizu, Japan; and a Research Fellow with The Hong Kong Polytechnic University. He is currently a Pearl River Scholarship Distinguished Professor and the Vice Dean of the School of Computer Science, Guangzhou University, China, where he is also the Director of Institute of Computer Networks. His research interests include artificial intelligence, big data, cloud computing, and cyberspace security. He is a Distinguished Member of CCF, and a member of ACM and IEICE.

MD. ZAKIRUL ALAM BHUIYAN received the Ph.D. degree. He was an Assistant Professor with Temple University. He is currently an Assistant Professor with the Department of Computer and Information Sciences, Fordham University, NY, USA, and the Founding Director of Fordham Dependable and Secure System Laboratory (DependSys). He is also a Visiting Professor with Guangzhou University, China. His research focuses on dependability, cybersecurity, big data, and cyber physical systems. His work in these areas published in top-tier venues, including the IEEE TC, TPDS, TDSC, TII, COMMAG, the IoT-J, ACM TOSN, TAAS, CS, INS, JNCA, and so on. He is a member of ACM. He has served as a Guest/Associate Editor for the IEEE TBD, ACM TCPS, the IoT-J, INS, FGCS, JNCA, and so on. He has also served as an Organizer, a General Chair, a Program Chair, a Workshop Chair, and a TPC Member of various international conferences, including the IEEE INFOCOM.